METALLIC MICRO HEAT EXCHANGERS: PROPERTIES, APPLICATIONS AND LONG TERM STABILITY

J.J. Brandner[1], W. Benzinger, U. Schygulla, S. Zimmermann and K. Schubert

Forschungszentrum Karlsruhe, Institute for Micro Process Engineering (IMVT),
P.O.Box 3640, DE-76021 Karlsruhe, Germany
[1] corresponding author: Phone +49 7247 82 3963, Fax +49 7247 82 3186,
e-mail: juergen.brandner@imvt.fzk.de

ABSTRACT

Micro heat exchangers, which until recently have been implemented only at laboratory scale, are now being available for industrial applications. They are well known for their superior heat transfer properties due to the large surface-to-volume ratio. But there are little data available on the long term stability of these devices.

In this paper application several application examples for micro heat exchangers made of stainless steel are presented. The devices consist of stainless steel foils providing numerous micro channels generated by mechanical micromachining or wet chemical etching. A number of the foils are arranged in a specific way and bonded together.

Device property descriptions as well as some possible application examples show the potential of metallic microstructure devices.

Results on two crossflow microstructure heat exchangers running in long term tests are presented. Both devices have been tested for more than 8000 hours each, using deionised water as test fluid. Experimental data on the heat transfer properties and the pressure drop are given and compared. It was found that the heat transfer capabilities were significantly decreased within the first few hundred hours of testing and then run into a saturation state. Performance degradation may be due to a fouling layer deposited on the heat exchange surface. Some other experimental applications in which fouling was expected to cause problems are described briefly.

INTRODUCTION

Since the early 90s, microstructure heat exchangers have been widely acknowledged as excellent tools for laboratory research, but only as a niche product for industrial applications. More recently, microstructure heat exchangers have been designed, manufactured and tested that provide the potential for industrial use.

To design those devices, conventional pre-calculation techniques like simple fluidmechanical equations based on the Nusselt theory can be used, as it was shown by Halbritter et al. (2004). Beside this, Wenka et al. (2000)

showed that CFD calculations may be advantageous to use for the primary design and to obtain a first idea of the heat transfer performance of such microstructure devices. Nevertheless, the manufacturing process is determined by the possibilities to obtain micro channels or microstructures, the bonding methods and of course by the needs of the processes the devices are meant for. Moreover, the process itself is limited by the long term stability of the microstructure devices against corrosion, blocking and fouling.

In this paper, the design and manufacturing technique of microstructure heat exchangers is described. Examples of microstructure heat exchangers and their potential are given by experimental results. Experimental results for the long term stability of two crossflow type microstructure heat exchangers are given in detail. Some more experimental results with regard to fouling and long term stability obtained with the same or other designs of microstructure heat exchangers are presented. A summary and short outlook complete the paper.

MANUFACTURING

Most processes running outside of a laboratory will need considerably high pressure resistance as well as resistance against corrosion. This means that the use of silicon as base material is not longer a suitable choice. Metallic microstructure heat exchangers are necessary to provide the demanded resistivity against pressure, temperature and corrosion. Therefore, it is necessary to choose a metal which can be microstructured quite easily and can also be bonded together to form stable and more or less complex structures. Due to the higher corrosion resistance, stainless steel is the first choice. Micro channels or other designs of microstructures in stainless steel foils may be obtained either by mechanical precision micromachining (e.g. milling, turning or drilling), as it is described by Schaller et al. (1999) or by wet chemical etching as described by Madou (2002). The cross section of the channels differs by the manufacturing method. While mechanically cut channels will take on the shape of the microtool used to cut, wet chemically etched micro channels have a semi-elliptic cross section due to the isotropic

etching effect. In Figure 1, a SEM photo of a mechanically cut microchannel foil with rectangular micro channels is shown, while Figure 2 shows a SEM picture of an etched microchannel stainless steel foil.

Depending on the manufacturing method, the surface quality differs. While mechanically cut microchannels in stainless steel provide an overall roughness of about 3 µm, wet chemically etched stainless steel microchannels show about three times this value – around 9 µm is common. This, of cause, is to be taken in account when fouling takes place.

To form the core of a microstructure heat exchanger, a number of microstructured foils is stacked together in the desired order and arrangement. The complete stack is then brought into a furnace and bonded by a diffusion bonding process. Depending on the material and the connecting face area, a strictly defined temperature and force program is applied to run the diffusion bonding process. The forces used for diffusion bonding are in the range from a few kN up to around 100 kN, depending on the connection area, while the applyable temperature range is from 500°C to more than 1,000°C.

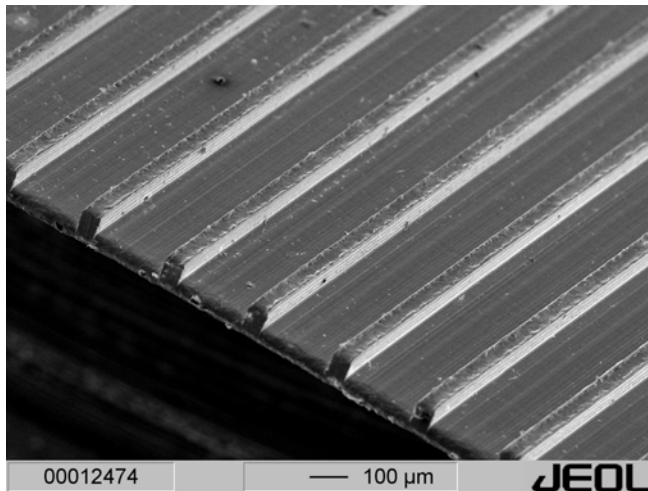The displacement of the micro channels can be reduced by aligning the single foils on one or more pins made to fit in holes in the corners of each foil.
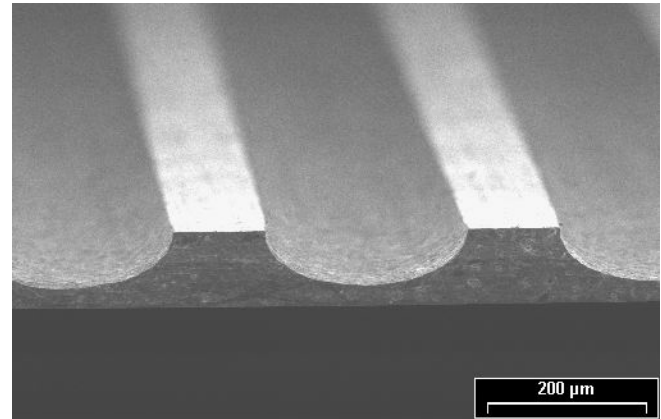

Fig. 2: SEM picture of a wet chemically etched microstructure foil. The semi-elliptic micro channels are about 200 µm wide and around 70 µm deep.

Fig. 1: SEM picture of a mechanically cut microstructure foil. The rectangular micro channels are 200 µm wide and around 100 µm deep.
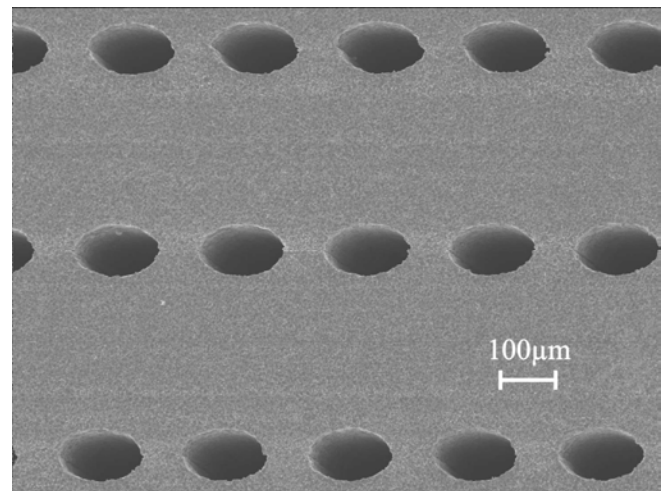

Fig. 3: SEM picture of full-elliptically shaped micro channels of a crossflow micro heat exchanger. The good alignment is clearly to see.

For microstructure foils, two possibilities for stacking exist: either the simple stacking (called "face-to-back"), or to stack them "face-to-face". Those two possibilities are of special interest for wet chemically etched micro channels, were the "face-to-back" version will form semi-elliptically shaped micro channels with small hydraulic diameters, while the "face-to-face" option can be used to generate full-elliptically shaped micro channels, as shown in Figure 3.

After the diffusion bonding step, the microstructure device is similar to a monolithic structure, as shown in Figure 4, where the micro channel system of a crossflow heat exchanger is shown. The second passage is laying across the visible face areas of the channels.
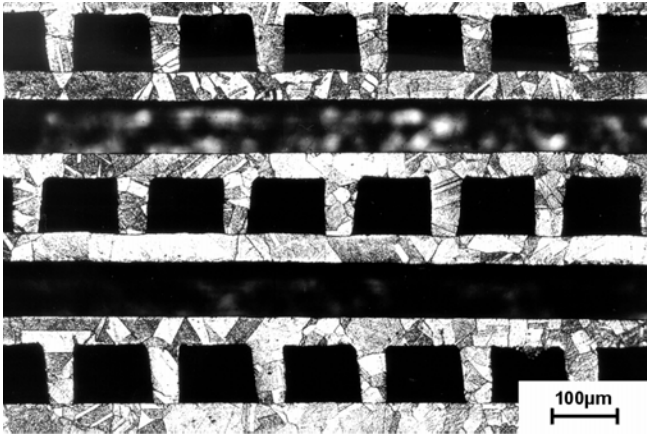
Fig. 4: Crossflow microstructure heat exchanger made of stainless steel after diffusion bonding. Only small hints of the single layer structure are visible.

The core bodies of the microstructure devices are cleaned and welded into a housing by electron beam welding. The housing may be equipped either with conventional tube fittings or any other fitting system suitable for the desired application. In Figure 5, an example photo of a crossflow heat exchanger core with an active volume of 1 cm³ and another device welded to standard fittings is shown.

Fig. 5: Core of a stainless steel crossflow microstructure heat exchanger (left) and a similar core welded to conventional tube fittings. The active heat transfer volume of both devices is 1 cm³.

Throughout the complete manufacturing process a quality control is stringent, e.g. measurements are made of the leak tightness, the overpressure resistance and other parameters. A more extensive description of manufacturing of microstructures and microstructure devices can be found in Brandner et al. (2006a).

PRECALCULATION AND MODELING

As mentioned above, for most devices the pre-calculation using standard Nusselt theory equations is suitable in many cases. Therefore, the hydraulic diameter of each microchannel can be calculated using the simple equation

$$d_h = \frac{4 \cdot F}{C} \tag{1}$$

where d_h is the hydraulic diameter, F is the cross section area of the channel and C is the circumference of the micro channels.

For further calculations with non-circular channels, a correction factor has to be applied to approximate a circular cross section. Those factors may be found, e.g., in VDI Wärmeatlas (1994). For the pressure drop, equations like the Darcy equation for laminar flow with a Reynolds number Re lower than approx. 2300 or an equation developed by Petukhov and Gnielinski for turbulent flow with a Reynolds number Re between 3000 and 10^5 may be applied (see VDI-Wärmeatlas (1994)).

For a microstructure heat exchanger having a defined geometry and known mass flows as well as inlet and outlet temperatures, the heat transfer therefore was calculated by the power balance equation (2).

$$\dot{m} \cdot c_p \cdot \Delta T = k \cdot A \cdot \Delta \vartheta_m \tag{2}$$

Here, $\dot{m}$ is the mass flow, c_p the specific heat capacity, ΔT the temperature difference, k the overall heat transfer coefficient, A the heat transfer area and $\Delta \vartheta_m$ the mean logarithmic temperature difference.

The effective heat transfer area A was calculated by

$$A = n_f \cdot n_{Ch} \cdot C \cdot l \tag{3}$$

were n_f is the number of microstructured foils, n_{Ch} is the number of microchannels per foil, C is the circumference of each microchannel and l is the length of the microchannels. $\Delta \vartheta_m$ was calculated from the formula given in VDI-Wärmeatlas (1994).

The heat transfer coefficient was defined for both a cold and a hot passage providing the same heat transfer area

like it is shown in equation (4), in which α is the heat transfer coefficient, Nu is the Nusselt number and λ_{Fluid} is the thermal conductivity of the fluid. Then, the overall heat transfer coefficient k was calculated using equation (5) with s being the foil thickness.

$$\alpha = \frac{Nu \cdot \lambda_{Fluid}}{d_h} \tag{4}$$

$$\frac{1}{k} = \frac{1}{\alpha_{hot}} + \frac{1}{\alpha_{cold}} + \frac{s}{\lambda_{solid}} \tag{5}$$

For laminar flow (Re < 2300), the Nusselt number was calculated using equations (6) to (9), where Pr is the Prandtl number.

$$Nu_{lam} = \sqrt[3]{\left(Nu_1^3 + 0.7^3 + \left(Nu_2 - 0.7\right)^3 + Nu_3^3\right)} \tag{6}$$

$$Nu_1 = 3.66 \tag{7}$$

$$Nu_2 = 1.615 \cdot \sqrt[3]{Re \cdot Pr \frac{d_h}{l}} \tag{8}$$

$$Nu_3 = \left(\frac{2}{1 + 22 \cdot Pr}\right)^{1/6} \cdot \sqrt{Re \cdot Pr \frac{d_h}{l}} \tag{9}$$

For turbulent flow (Re > 2300), the Nusselt number was defined by equations (10) to (11). Here, ξ is a form factor (see VDI Wärmeatlas (1994)).

$$Nu_{turb} = \frac{\frac{\xi}{8} \cdot (Re - 1000) \cdot Pr}{1 + 12.7 \cdot \sqrt{\frac{\xi}{8} \cdot \left(Pr^{2/3} - 1\right)}} \cdot \left(1 + \left(\frac{d_h}{l}\right)^{2/3}\right) \tag{10}$$

$$\xi = \left(1.82 \cdot \log(Re) - 1.64\right)^{-2} \tag{11}$$

When fluids with similar specific heat capacity are applied to both passages, the heat transfer efficiency ε can be used easily for comparison of differently designed (microstructure) devices. A definition is given in equation (12) or can be taken from VDI Wärmeatlas (1994) or Wagner (1999).

$$\varepsilon = \frac{\dot{Q}}{\dot{m} \cdot c_{mean} \cdot \left(T_{hot,in} - T_{cold,in}\right)} \tag{12}$$

In equation (12), $\dot{Q}$ is the thermal power, $\dot{m}$ the mass flow, T the temperature defined by the subscripts and c_{mean} the mean specific heat capacity.

In the specific case of symmetric fluid flow and using the same fluid for both passages, the capacity flow of both fluids is almost the same. Then, equation (12) can be rearranged to calculate the heat transfer efficiency ε with equation (13), which is given in VDI Wärmeatlas (1994).

$$\varepsilon = \frac{T_{cold,out} - T_{cold,in}}{T_{hot,in} - T_{cold,in}} \tag{13}$$

For modeling of the microstructure devices, either the commercially available CFD software FLUENT or the simple Nusselt theory equations have been used. With these equations, a complete microstructure device, which means the plenum outlet temperature at a certain mass flow, was precalculated. Using FLUENT, a temperature distribution for a system consisting of two microchannel foils only was performed and therefore the temperature distribution across the complete area of the foils was calculated, as it is described by Halbritter et al. (2004) and Schubert et al. (2001).

In Figure 6 an example for the temperature distribution obtained for an arrangement of two crossflow microstructure heat exchanger foils is shown. Here, an asymmetric mass flow of $50 \, \text{kg} \cdot \text{h}^{-1}$ for the cold water passage and $700 \, \text{kg} \cdot \text{h}^{-1}$ for the hot water passage was assumed. The temperature distribution was calculated and plotted as function of the distance from the inlet and the channel number.

DEVICE PROPERTIES AND APPLICATIONS

Microstructure devices manufactured in the described way provide unique properties. After the diffusion bonding, a monolithic device core is generated out of single metallic foils. Thus, the devices are stable against high pressures due to the plane connection between the single foil layers. Pressure resistance up to 100 MPa at room temperature is possible, as it is described by Schubert et al. (2001). The devices can be scaled to the desired mass flow range, reaching from some grams up to several tons liquid per hour and passage of the device. The pressure drop resulting on the microstructure passages is in the range of up to 1 MPa, depending on the density and viscosity of the fluid.
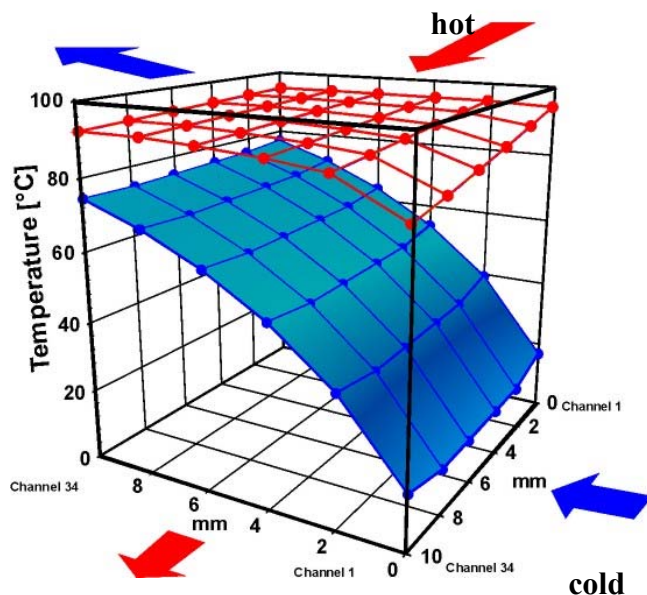
Although one of those devices is running continuously within a production facility for more than one year, we could not observe any fouling inside the microstructure system yet.

Fig. 6: Temperature distribution inside a two foil crossflow arrangement at an asymmetrical water mass flow ($50 \, \text{kg} \cdot \text{h}^{-1}$ cold water, $700 \, \text{kg} \cdot \text{h}^{-1}$ hot water mass flow), calculated using FLUENT.

By parallelization of the devices, mass flow ranges of some tons per hour and per passage can be reached. In Fig. 7, a stack of five crossflow heat exchanger devices is shown. With this stack, a maximum mass flow of 35 tons of water per passage and per hour is possible. Thus, a maximum thermal power of up to 1 MW can be transferred.

Devices providing an active volume of 1 cm^3 can transfer a thermal power of up to 20 kW, measured with water of 95°C in one passage and water of 8°C in the other, at a mass flow of about 700 kg/h each, as it is reported by Brandner et al. (2006b). The overall heat transfer coefficient k of the devices with linear microchannels is in the range of $20 \, \text{kW/(m}^2 \cdot \text{K)}$ and can be increased to values about $56 \, \text{kW/(m}^2 \cdot \text{K)}$ and more by changing the design of the microchannels. A surface-to-volume ratio of up to $30000 \, \text{m}^2/\text{m}^3$ can be provided, corresponding to Brandner et al. (2006b).

With an electrically powered stainless steel heat exchanger device, a biodiesel flow is continuously heated from 80°C to 105°C at a mass flow of 1000 kg/h, as it is presented in Rinke et al. (2006). The manufacturing and working principle of the device is given by Henning et al. (2004). In Fig. 8, an electrically powered microchannel device used for this application is shown, providing a maximum electrical power of 20 kW.

Fig. 7: Stack of five crossflow microchannel heat exchangers. 1 MW thermal power can be transferred at a water mass flow of 35 tons per hour and per passage.

Fig. 9 shows a specially designed chemical modular microstructure reactor for the production of fine chemicals. This device was developed in cooperation with the DSM company and was used in several campaigns in commercial production. At a maximum reactant mass flow of 1700 kg/h, a thermal power of several hundred kW could be transferred within a number of crossflow microchannel heat exchanger modules. They have been combined with a number of specially designed micro mixers to provide fast and

sufficient mixing and temperature control for the reaction. More details can be found in Kraut et al. (2006).

More examples for applications are given in literature, e.g. in Hessel et al. (2006).

Fig. 8: Electrically powered microchannel heat exchanger used to heat a production mass flow of 1000 kg/h biodiesel.

Fig. 9: Microstructure reactor for chemical production. In cooperation with the company of DSM, this device was developed and manufactured. It is about 650 mm long and weighs 290 kg. Several thousand microstructures are integrated to provide excellent mixing and heat transfer.

EXPERIMENTAL SETUP

For experimental tests of microstructure heat exchangers a test system with hot and cold water as fluids, ducted in closed loops, was used. Metal frit filters were used to clean the water from particles. Results of a water analysis are given in Table 1.

The system was made from conventional components as far as it was possible. The pumps were conventional centrifugal pumps generating a maximum pressure of up to 1.6 MPa and covering a throughput range from $5 \text{ kg} \cdot \text{h}^{-1}$ up to $1000 \text{ kg} \cdot \text{h}^{-1}$. Throughputs in the range from $0.4 \text{ kg} \cdot \text{h}^{-1}$ to $6 \text{ kg} \cdot \text{h}^{-1}$ can be realized by the use of HPLC pumps.

For the hot water loop, an electrical heater with a heating power of 30 kW was used. For low throughputs, an electrically powered microstructure flowthrough heater was applied directly in front of the microstructure heat exchanger to be tested. This was necessary to provide a constant inlet temperature.

For the cold water loop, a plate heat exchanger with a maximum power of 30 kW was used. The temperatures of the loops are set to 10°C and 95°C, measured at the inlet of the micro heat exchanger, at a pressure of 0.9 MPa.

The mass flow through the microstructure heat exchangers are coarsely set by a bypass valve adjustment. A fine trimming is done by mass flow controllers.

Table 1. Chemical analysis results of water used in the experimental setup.

total electrical conductivity	30.55	μS/cm
Ca	2.400	mg/l
Mg	1.610	mg/l
Al	0.040	mg/l
Mn	0.031	mg/l
Cu	0.029	mg/l
Zn	0.085	mg/l

The sensors used in the test rig are membrane pressure transducers with an accuracy of 0.25% of the end value (range: $0 - 1.6$ MPa), PT100 resistance sensors with a resolution of 0.7 K, Type K thermocouples with a resolution of 1 K and mass flow meters based on the Coriolis principle. The accuracy of the mass flow meters is 1% o.r. for the flow range up to $10 \text{ kg} \cdot \text{h}^{-1}$ and decreasing to about 0.03% o.r. for $100 \text{ kg} \cdot \text{h}^{-1}$ and above. A schematic view of the test system is shown in Figure 10.
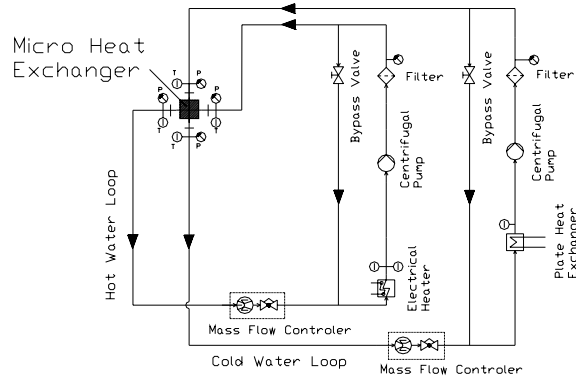
Fig. 10: Schematic view of the test system for microstructure heat exchangers.

With this setup, microstructure heat exchangers are tested in a symmetrical way, which means the mass flow through the hot and cold water passage is kept at an almost constant value for a certain time. Plenum temperatures and pressures at the inlet and the outlet of each passage are measured. The data are saved in a computerized data archiving system using LABView software. For each microstructure heat exchanger, the mass flow is increased as high as possible, e.g. up to a level where the pressure drop measured over one passage has reached a value around 0.8 MPa. The experiments have been done at least twice (one time with increasing mass flow, one time with decreasing mass flow) to obtain consistent data and to exclude hysteresis effects.

EXPERIMENTAL RESULTS

Results for different experiments with crossflow microchannel devices as well as electrically heated devices are given in the following section.

Comparison of Crossflow Microstructure Heat Exchangers

In this section the focus is set to the comparison of two crossflow microstructure devices with an active volume of 1 cm^3. The design data for those devices are given in Table 2. Both devices have been used for several thousand hours in long term run within the experimental setup shown above.

For both devices, integral measurements have been taken. the maximum mass flow per passage as well as the

pressure drop over the hot and cold water passage at different mass flow values have been taken as function of the time. From this, the transferred thermal power and the overall heat transfer coefficient at the same mass flow values have been calculated as function of time.

Table 2: Technical data of the crossflow microstructure heat exchangers compared in this publication.

	66082	1246
channel cross section	rectangular	fully elliptic
channel dimensions (width, height, length)	200 μm 100 μm 14 mm	160 μm 100 μm 14 mm
hydraulic diameter	133 μm	121 μm
number of channels per passage	850	1118
effective heat transfer area	0.0051 m^2	0.00868 m^2
material: W316L, heat conductivity: 15 W / m· K		

Unfortunately, it was not possible to look inside the microstructure heat exchangers without destroying them. Thus, although it can be seen from the measurement values that some performance degradation occurred probably due to fouling inside the microchannel system, it was not possible to confirm this.

Experimental Results for the Comparison of Crossflow Heat Exchanger Devices. Fig. 11 presents the maximum mass flow plotted over the time for both the hot and the cold water passage of the rectangular channel device. It is clearly to see from Fig. 11 that within the first 1000 hours a significant decrease of the maximum applyable mass flow is shown, which takes place in both passages simultaneously. After about 1600 hours of operation, the maximum mass flow is almost constant.

Fig. 12 presents the same data for the fully elliptic channel device. Here, the maximum mass flow in the cold water passage is almost constant, while the maximum mass flow through the hot water passage decreases significantly within the first 600 hours of operation, and is then slowly increasing again. This gives a clear hint that there has to be some fouling inside the hot water passage, since the

experimental setup was not changed and worked perfectly within the normal uncertainty ranges.
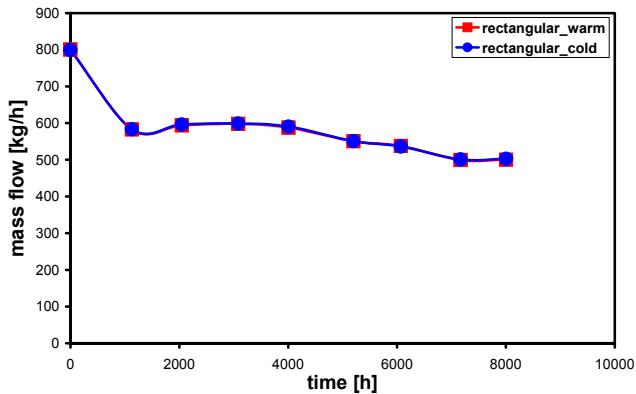

Fig. 11: Maximum mass flow in both passages of the rectangular channels device, plotted versus the total operation time. The plots are laying above eachother.

In Fig. 13, the pressure drop measured over the hot water passage and the cold water passage of the elliptic channel device is given for a mass flow of 200 kg/h and 100 kg/h, plotted versus the total operation time. The steep increase of the hot waters pressure drop indicates some kind of fouling taking place inside the hot water passage, while only a small increase along the time is seen for the cold water passage.
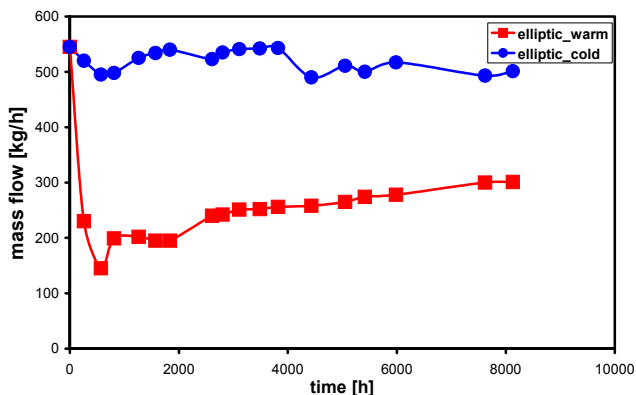

Fig. 12: Maximum mass flow in both passages of the elliptic channels device, plotted versus the total operation time.
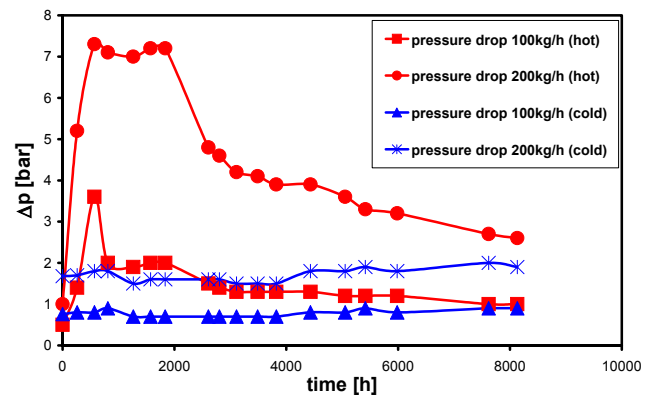

Fig. 13: Pressure drop plot versus the total operation time for the hot and cold water passage of the elliptic channel device.

The processes happening inside the hot water passage seems to be reversible, since the maximum water mass flow as well as the pressure drop starts to recover slowly with increasing operation time. This can be seen in Fig. 12 and Fig. 13. It is not clear yet whether the original values will be reached anymore, but the experiment is still running, and measurements are taken every 1000 hours of operation time. Nevertheless, it is very unlikely that the values will recover to the starting point values.

In Fig. 14, the overall heat transfer coefficients for the rectangular and the elliptic device are shown, plotted versus the total operation time. The values for two mass flows are presented, 100 kg/h and 200 kg/h of the warm water passage. It is clearly to see that the overall heat transfer coefficient is reduced drastically within the first few hundred hours of operation and then remains almost constant for the complete operation time. Thus, the heat transfer capabilities of the devices are first reduced by about 5% to 10%, but then kept at this level. No further decrease is shown.

Crossflow Heat Exchangers for Bio-Technology

Within a first study, a stainless steel crossflow heat exchanger was tested for its suitability to instantaneously cool down a sample flow of a mammalian cell culture suspension from 37°C to 0°C by the use of a mixture of ethylene glycol and water as cooling fluid. This was necessary to almost stop the cell metabolism and to analyse the metabolites inside the cells. In Fig. 15, the temperature dependency of molar densities of four metabolites plotted against the temperature are given as examples. Here it is clearly to see that with increasing sample temperature the molar mass of metabolites is decreasing in the most cases.

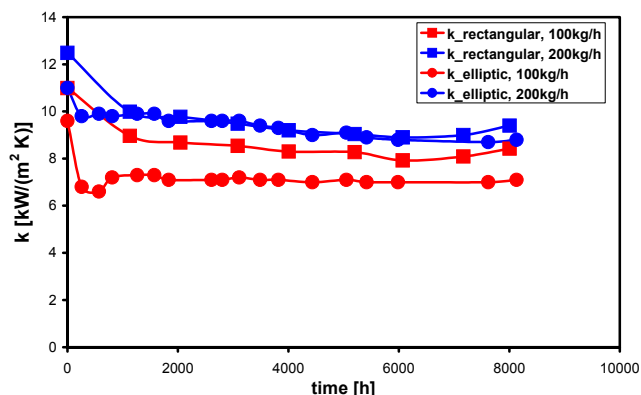Thus, to observe the intracellular density, a snapshot-like sampling and analysis procedure is necessary.

Fig. 14: Overall heat transfer coefficient k for the rectangular and the elliptical channels device, plotted versus the operation time, for two different mass flow values.

It was not clear whether a large number of the cells will be damaged by the heat exchanger or fouling of the microchannels will take place due to the agglomeration of the cells within the suspension. Moreover, it was not clear whether the heat exchanger could be cleaned well enough to run the device for more than only one cell sample or different cell culture types.

Experimental Results with a Crossflow Heat Exchanger for Bio-Technology. Within the study, Wiendahl et al. (2007) showed that the number of disrupted cells is negligible small and, thus, the heat exchanger is suitable for cell culture sampling. No relevant fouling or blocking was observed while the samples have been taken, and no cell agglomeration was found. Moreover, cleaning and fumigation was easy to perform with conventional methods like, for example, an autoclave. It was shown that the sampling method is suitable for gathering relevant intracellular concentration data with a precision not known yet. Thus, micro heat exchangers provide great advantages compared to the standardized sampling methods.

Other Experiments

Other experiments with microstructure devices have been performed. A crossflow heat exchanger was used in a side-arm of the wastewater cleaning facilities of the Karlsruhe Research Center. For a couple of months, a small part of the waste water running from the facilities to the

environment after cleaning was ducted through a metal mesh filter and then through the micro heat exchanger. No significant fouling was observed.
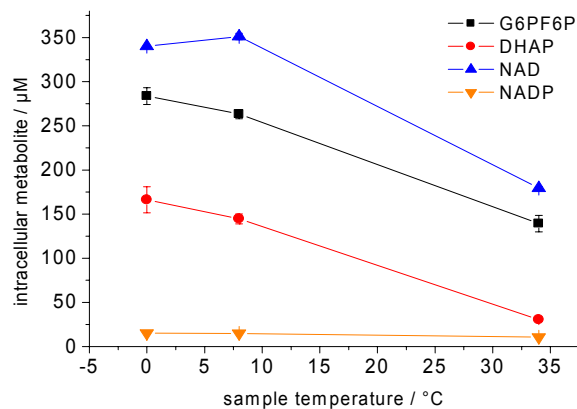

Fig. 15: Dependency of the intracellular density of four cell metabolites against the sampling temperature.

A special type of electrically powered device was tested with a defined solution of $CaCO_3$. The device was running in a test loop, heating it up to a temperature of 80°C for two minutes and cooling it down again then. This was repeated several tens of thousand times. After about 60 kg of the $CaCO_3$ solution was pumped through the device, the pressure drop increased significantly and the heat transfer opportunities was decreased significantly by a deposited calcination fouling layer. Thus, a cleaning step was arranged, using conventional citric acid to clean the device. After this step, the experiment could be continued and the device was regenerated completely.

Some more experiments are still running. More results about fouling in microstructure devices, prevention of fouling and possible cleaning methods are expected in near future.

CONCLUSIONS

Fouling and blocking in microstructure devices is definitely a point to keep in mind. The microstructures may be in the same size range as blocking particles are. Generation of fouling films inside of microstructure systems may lead not only to less performance with respect to heat transfer but also to complete blocking and, thus, the possibility of a non-working device as can happen in conventionally sized heat exchangers.

Unlike those, most microstructure devices can not be disassembled and cleaned as single parts. Thus, on-stream cleaning procedures have to be developed.

There are certain countermeasures for conventional devices dealing with fouling and blocking, such as filters, protective layers, etc. Some of those may also be useful for microstructure devices, some are not applicable. Due to the huge variety of different sizes, types, manufacturing methods and applications of microstructure systems, there are lots of different more or less important points to deal with when talking about long term stability.

Like with the corrosion resistance, it has to be taken in account that the restraints and limitations are different from those existing for conventional sized devices, and, thus, new regulatories have to be generated. Moreover, special designs have to be developed and applied to prevent fouling inside microstructure devices.

OUTLOOK

For fouling and blocking in microstructure devices as well as for their long term stability, new design concepts and manufacturing methods as well as integrated countermeasures could lead to a significant better acknowledgement of this technology in the industry. In many cases, not only a lack of experimental data but also the fear to run into difficulties generated by fouling in microstructures often prevents the use of these high-performance devices. Overcoming this restraints will be one of the most important tasks in the development of microstructure devices for the next few years.

NOMENCLATURE

Latin symbols

A	effective heat transfer area	m^2
C	microchannel circumference	m
F	microchannel face area	m^2
Nu	Nusselt number	
Pr	Prandtl number	
$\dot{Q}$	thermal power	W
Re	Reynolds number	
T	temperature	K, °C
c_{mean}	mean specific heat capacity	$J \cdot kg^{-1} \cdot K^{-1}$
c_p	specific heat capacity	$J \cdot kg^{-1} \cdot K^{-1}$
d_h	hydraulic diameter	m, μm
k	overall heat transfer coeff.	$W \cdot m^{-2} \cdot K^{-1}$
l	microchannel length	m
$\dot{m}$	mass flow	$kg \cdot h^{-1}$
n_{Ch}	number of microchannels per foil	
n_f	number of microstructured foils per passage	
s	path length, foil thickness	m

Greek symbols

α	heat transfer coefficient	$W \cdot m^{-2} \cdot K^{-1}$
λ	thermal conductivity	$W \cdot m^{-1} \cdot K^{-1}$
ε	heat transfer efficiency	%
$\Delta \vartheta_m$	mean logarithmic temperature difference	K
ξ	form factor	

Subscripts

cold	cold water passage
fluid	specified fluid
hot	hot water passage
in	inlet position
lam	laminar
out	outlet position
solid	solid material
turb	turbulent

REFERENCES

Brandner, J.J., Microfabrication in Metals and Polymers, in: *Advanced Micro- and Nanosystems Vol.5,* eds. Korvink et al., Wiley-VCH, Weinheim, Germany, 2006, pp. 267-320

Brandner, J.J., Anurjew, E., Bohn, L., Hansjosten, E., Henning, T., Schygulla, U., Wenka, A., Schubert, K., 2006, Concepts and Realization of microstructure heat exchangers for enhanced heat transfer, *Experimental Thermal and Fluid Science* 30, 801-809 (2006)

Halbritter, A., Schygulla, U., Wenka, A. and Schubert, K., 2004, Comparison of Numerical Simulation and Experimental Results for Crossflow and Counterflow Microchannel Heat Exchangers, *Proc., 2nd Int. Conf. On Microchannels and Minichannels, S.G. Kandlikar et al., eds., ASME, New York, N.Y. 10016, USA, pp.967-975*, 2004

Henning, T., Brandner, J.J., Schubert, K., 2004, Characterisation of electrically powered micro heat exchangers, *Chem. Eng. J.* 101/1-3, 339-345 (2004)

Hessel, V., Hardt, S., Löwe, H., 2005, Chemical Micro Process Engineering 1+2, Fundamentals, Modelling and Reactions / Processes and Plants, Wiley-VCH, Weinheim, Gemany, 2005

Kraut, M., Bohn, L., Wenka, A., Schubert, K., Successful Upscale of laboratory micro reactor into industrial scale, 2006, *Proc. 6th ANQUE Int. Congress of Chemistry "Chemistry and Sustainable development" 2006*, Gráficas DEVA, Spain, T2-L-9, 315-316

Madou, M, 2002, *Fundamentals of Microfabrication*, 2nd ed, CRC Press LLC, Boca Raton, FL, USA, 2002

Rinke, G., Kerschbaum, S., Wenka, A., Holpe, H., Micro process engineering for industrial production of biodiesel, 2006, *Proc. 9th Int. Conf. on Micro Reaction Eng. (IMRET 9) 2006*, 257-258

Schaller, Th., Bohn, L., Mayer, J., Schubert, K., 1999, Microstructure grooves with a width of less than 50µm cut with ground hard metal micro end mills, *Precision Eng. 23, 1999,* 229-235

Schubert, K., Brandner, J.J., Fichtner, M., Linder, G., Schygulla, U., Wenka, A., 2001, Microstructure devices for applications in thermal and chemical process engineering, *Microscale Thermophysical Engineering, 5, 2001,* 17-39

VDI Wärmeatlas, 7.ed., VDI-Verlag, Düsseldorf, Germany, 1994

Wagner, W., 1999, Wärmeaustauscher, 2nd ed., Vogel-Verlag, Würzburg, Germany, 1999

Wenka, A., Fichtner, M. and Schubert, K., 2000, Investigations of the Thermal Properties of a Micro Heat Exchanger by 3D Fluid Dynamics Simulation, *Proc., 4th Int. Conf. on Microreaction Technology,* I. Rinard et al., eds., AIChE, 2000, 256-263

Wiendahl, C., Brandner, J.J., Küppers, C., Luo, B., Schygulla, U., Noll, T., Oldiges, M., 2007, A Microstructure Heat Exchanger for Quenching the Metabolism of Mammalian Cells, *Chem. Eng. Technol. 2007*, 30, No. 3, 1-8